Materials Research Proceedings **26** (2023) 499-504 https://doi.org/10.21741/9781644902431-81

Two-scale asymptotic homogenization of hierarchical locally resonant metamaterials in anti-plane shear conditions

David Faraci[1,a *], Claudia Comi[1,b] and Jean-Jacques Marigo[2,c]

[1] Department of Civil and Environmental Engineering, Politecnico di Milano, Milan, Italy

[2]Laboratoire de Mécanique des Solides, Ecole Polytechnique, Palaiseau, France

[a] david.faraci@polimi.it, [b] claudia.comi@polimi.it, [c] jean-jacques.marigo@polytechinque.edu

Keywords: Homogenization, Local Resonance, Band Gaps

Abstract. Local resonant metamaterials are a class of microstructured man-made material which attenuate the propagation of waves in certain frequency ranges, known as band gaps. In this work, we study through asymptotic homogenization the anti-plane shear wave propagation in metamaterial with a stiff matrix and soft inclusions, periodically distributed, which present a hierarchical geometry. Band gaps of the metamaterial are then analytically predicted by the intervals of frequency in which the effective mass becomes negative.

Introduction

Metamaterials have attracted a lot of interest in dynamic problems due to their peculiar and unusual properties related to wave propagation. A particular class of these materials are the locally resonant metamaterials (LRMs), which are specifically designed to trap the energy of propagating waves by employing the mechanism of local resonance. The frequency intervals in which waves are attenuated are known as band gaps.

Typically, LRMs have a periodic structure, made of one or several phases, hence the Bloch theorem [1,2] can be employed to reconstruct their band structure, including band gaps, in the linear-elastic regime.

In recent years, several researchers propose hierarchical geometries for LRMs to obtain wider band gaps [3,4]. Numerical simulations of a continuum system exhibiting a hierarchical geometry may represent a huge computational burden and analytical predictions of their dynamical properties are mainly restricted to discrete systems of lumped masses and springs.

Two-scale asymptotic homogenization is a promising technique which can be used to study the dynamic effective behaviour of metamaterials [5,6]. This method has been employed to study a periodic LRM made of a connected stiff matrix and soft inclusion in two- and three-phase solids [7,8], and in thin plates [9], allowing the identification of band gaps as the intervals of negative effective dynamic mass.

In this work, we extend the results obtained in [8], to study the anti-plane shear wave propagation in a three-phase hierarchical LRM constituted by a connected matrix with a periodic repetition of coated inclusions which are in turn microstructured, thus realizing a hierarchical LRM. In particular, we consider the presence of several concentrical annular rings of rigid masses, with interposed soft coatings, in each inclusion. The effective mass of the metamaterial, which is frequency-dependent, is derived up to the solution of a tridiagonal linear system. The analytical predictions of band gaps are validated by comparison with those obtained by numerical Bloch-Floquet analyses. Finally, some parametric studies are performed to show the potentiality of the proposed approach for the design and optimization of hierarchical LRMs.

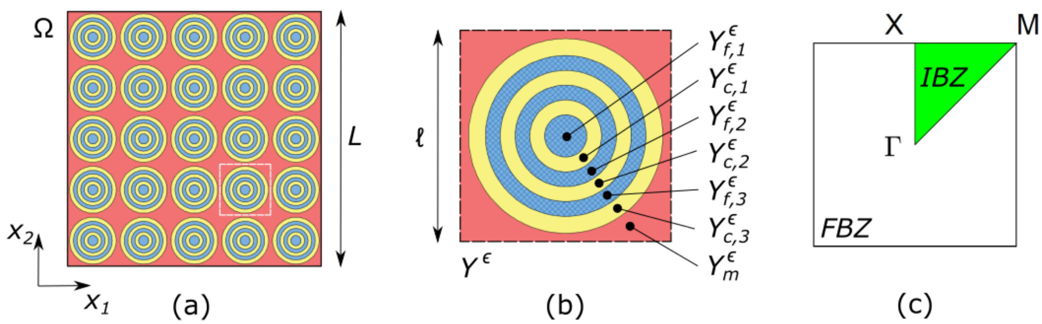

Figure 1: (a) Geometry of the hierarchical metamaterial with its (b) unit cell composed by the matrix (red), coatings (yellow) and rigid masses (blue) in the case $N = 3$. (c) First and Irreducible Brillouin zone of the square lattice.

Two-scale asymptotic homogenization

We consider a three-dimensional heterogeneous linear-elastic media which is characterized by a two-dimensional periodicity. The cross-section Ω of the body, shown in Fig. 1a and having characteristic size L, is made of a connected stiff matrix (*m*) and several inclusions periodically distributed. Each inclusion presents a hierarchical geometry consisting of N concentric annular rigid masses (*f*) with interposed soft coatings (*c*). The unit cell Y^ϵ of the periodic media, depicted in Fig. 1b with its characteristic size ℓ, shows the domains $Y^\epsilon_{f,\alpha}$ and $Y^\epsilon_{c,\alpha}$ of each rigid mass and coating, which are numbered from the innermost to the matrix Y^ϵ_m by $\alpha = 1,\ldots,N$.

Under the hypothesis of separation of scales, i.e., when $\epsilon = \ell/L \ll 1$, the effective behaviour of the metamaterial can be described through asymptotic homogenization.

The anti-plane shear wave propagation problem is governed by the scalar Helmholtz equation

$$\mathrm{div}(\mu^\epsilon \nabla w^\epsilon) + \rho^\epsilon \omega^2 w^\epsilon = 0 \qquad \text{in}\ \Omega\ , \tag{1}$$

where w^ϵ is the out of plane displacement and ω is the angular frequency of the propagating wave. The terms μ^ϵ and ρ^ϵ in Eq. 1 are the periodically varying shear modulus and mass density of the materials, which are assumed to be μ_m, ρ_m for the matrix, $\epsilon^2 \mu_c, \rho_c$ for the coatings and ρ_f for the rigid masses, with μ_m and ρ_m of the same order of magnitude of μ_c and ρ_c, ρ_f.

According to the two-scale homogenization technique, introducing the fast variable $\mathbf{y} = \mathbf{x}/\epsilon$ and the re-scaled unit cell $Y = Y^\epsilon/\epsilon$, the solution of Eq. 1 is searched in the form

$$w^\epsilon(\mathbf{x}) = w^0(\mathbf{x}, \mathbf{x}/\epsilon) + \epsilon w^1(\mathbf{x}, \mathbf{x}/\epsilon) + \ldots\ , \tag{2}$$

where the functions $w^i(\mathbf{x}, \mathbf{y})$ are defined on $\Omega \times Y$ and are periodic with respect to $\mathbf{y}$. Substituting Eq. (2) into Eq. (1) it is possible to prove that the 0-th order displacement in the matrix depend only on $\mathbf{x}$, i.e., $w^0(\mathbf{x}, \mathbf{y}) = W^0_m(\mathbf{x})$ in $\Omega \times Y_m$, see [7] for the full derivation.

Moreover, due to the radial symmetry of coatings and inclusions the masses rigidly translate within the unit cell. That means that $w^0(\mathbf{x}, \mathbf{y}) = \psi_\alpha W^0_m(\mathbf{x})$ in $\Omega \times Y_{f,\alpha}$ with $\psi_1, \ldots, \psi_\alpha$ unknown coefficients.

Materials Research Proceedings **26** (2023) 499-504 https://doi.org/10.21741/9781644902431-81

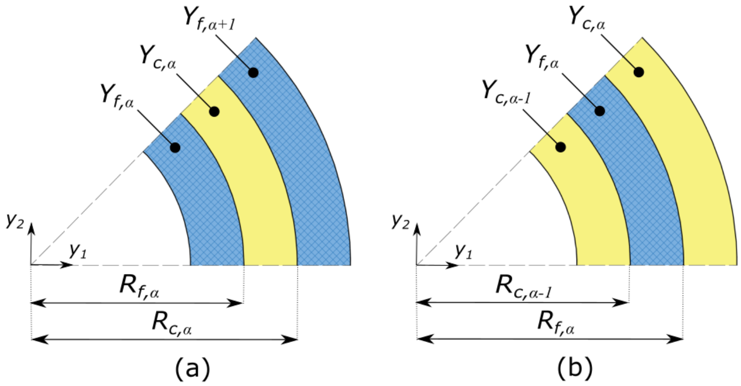

Figure 2: Detail of the circular sector of (a) the α-th coating surrounded by two rigid masses, and (b) the α-th rigid mass surrounded by two coatings.

Motion of the coatings. Restricting Eq. 1 at order ϵ^0 in the α-th coating, one obtains

$$\mu_c \Delta_{\mathbf{y}} w^0 + \rho_c \omega^2 w^0 = 0 \qquad \text{in } \Omega \times Y_{c,\alpha}, \tag{3}$$

with proper boundary conditions to guarantee the continuity of the solution at interfaces. For $\alpha \neq N$, as shown in Fig. 2a, these BCs read $w^0 = \psi_\alpha W_m^0$ on $\partial Y_{c,\alpha} \cap \partial Y_{f,\alpha}$ and $w^0 = \psi_{\alpha+1} W_m^0$ on $\partial Y_{c,\alpha} \cap \partial Y_{f,\alpha+1}$. Due to linearity the solution of Eq. 3 is given by $w^0(\mathbf{x},\mathbf{y}) = W_m^0(\mathbf{x})\eta_\alpha(\mathbf{y})$ in $\Omega \times Y_{c,\alpha}$. Using polar coordinates, one obtains a solution depending on the radial coordinate r only, in the form

$$\eta_\alpha(r) = \frac{J_0(\lambda r)Y_0(\lambda R_{c,\alpha}) - J_0(\lambda R_{c,\alpha})Y_0(\lambda r)}{J_0(\lambda R_{f,\alpha})Y_0(\lambda R_{c,\alpha}) - J_0(\lambda R_{c,\alpha})Y_0(\lambda R_{f,\alpha})}\psi_\alpha + \frac{J_0(\lambda R_{f,\alpha})Y_0(\lambda r) - J_0(\lambda r)Y_0(\lambda R_{f,\alpha})}{J_0(\lambda R_{f,\alpha})Y_0(\lambda R_{c,\alpha}) - J_0(\lambda R_{c,\alpha})Y_0(\lambda R_{f,\alpha})}\psi_{\alpha+1}. \tag{4}$$

In Eq. 4 J_p and Y_p are the p-order Bessel's functions of first and second kind, $\lambda^2 = \rho_c \omega^2 / \mu_c$, while $R_{c,\alpha}, R_{f,\alpha}$ are the external radius of the α-th coating and inclusion, see Fig. 2a. Note that this solution can be extended also for the N-th coating by setting $\psi_{N+1} = 1$.

Motion of the masses of the inclusions. Up to now, the 0-th order displacement w^0 is determined up to the knowledge of the matrix displacement W_m^0 and of the N constants ψ_α. The latter can be determined by enforcing the global dynamic equilibrium of each rigid mass. For the α-th mass the equilibrium reads

$$\mu_c \int_{\partial Y_{f,\alpha}} \frac{\partial w^0}{\partial r} ds + \rho_f |Y_{f,\alpha}| \omega^2 \psi_\alpha W_m^0 = 0. \tag{5}$$

If $\alpha \neq 1$, i.e., we are not considering the innermost mass (see Fig. 2b), Eq. 5 can be rewritten as

$$f_{\alpha-1}(R_{c,\alpha-1})\psi_{\alpha-1} + \left[g_{\alpha-1}(R_{c,\alpha-1}) - f_\alpha(R_{f,\alpha}) + \frac{\lambda^2 \rho_f}{2\rho_c}(R_{f,\alpha}^2 - R_{c,\alpha-1}^2) \right]\psi_\alpha - g_\alpha(R_{f,\alpha})\psi_{\alpha+1} = 0, \tag{6}$$

where we have introduced the functions

$$f_\alpha(r) = \frac{J_1(\lambda r)Y_0(\lambda R_{c,\alpha}) - J_0(\lambda R_{c,\alpha})Y_1(\lambda r)}{J_0(\lambda R_{f,\alpha})Y_0(\lambda R_{c,\alpha}) - J_0(\lambda R_{c,\alpha})Y_0(\lambda R_{f,\alpha})}\lambda r, \quad g_\alpha(r) = \frac{J_0(\lambda R_{f,\alpha})Y_1(\lambda r) - J_1(\lambda r)Y_0(\lambda R_{f,\alpha})}{J_0(\lambda R_{f,\alpha})Y_0(\lambda R_{c,\alpha}) - J_0(\lambda R_{c,\alpha})Y_0(\lambda R_{f,\alpha})}\lambda r. \tag{7}$$

The dynamic equilibrium of the innermost mass ($\alpha = 1$) is expressed again by Eq. 6 with $f_0 = g_0 = R_{c,0} = R_{f,0} = 0$. The system given by Eq. 6 written for $\alpha = 1, ..., N$ is a tridiagonal system which allows to compute the unknowns ψ_α for each value of λ, i.e., of ω.

Dispersion relation. Taking the average of Eq. 1 at order $\eth^0$ over the unit cell, one obtains the effective equation of motion of the hierarchical metamaterial

$$\mathrm{div}_{\mathbf{x}}(\boldsymbol{\mu}^0 \cdot \nabla_{\mathbf{x}} W_m^0) + \rho^0(\omega)\omega^2 W_m^0 = 0 \qquad \text{in } \Omega, \qquad (8)$$

where $\boldsymbol{\mu}^0$ is the positive definite effective stiffness tensor (see [7] for the detail of its derivation) and $\rho^0(\omega)$ is the frequency-dependent effective dynamic mass density, which expression is

$$\rho^0(\omega) = \rho_{st} + \frac{\rho_f}{|Y|}\sum_{\alpha=1}^{N} |Y_{f,\alpha}|(\psi_\alpha - 1) + \frac{\rho_c}{|Y|}\sum_{\alpha=1}^{N} |Y_{c,\alpha}|(F_\alpha \psi_\alpha + G_\alpha \psi_{\alpha+1} - 1). \qquad (9)$$

In Eq. 9, ρ_{st} is the static mass density and F_α, G_α are constants defined by

$$\begin{aligned} &\rho_{st} = \rho_m \frac{|Y_m|}{|Y|} + \rho_f \frac{|Y_f|}{|Y|} + \rho_c \frac{|Y_c|}{|Y|}, \\ &F_\alpha = \frac{2}{\lambda^2} \frac{f_\alpha(\lambda R_{c,\alpha}) - f_\alpha(\lambda R_{f,\alpha})}{R_{c,\alpha}^2 - R_{f,\alpha}^2}, \; G_\alpha = \frac{2}{\lambda^2} \frac{g_\alpha(\lambda R_{c,\alpha}) - g_\alpha(\lambda R_{f,\alpha})}{R_{c,\alpha}^2 - R_{f,\alpha}^2}. \end{aligned} \qquad (10)$$

Substituting into Eq. 8 the monochromatic wave $W_m^0(\mathbf{x}) = \exp(i\,\mathbf{k}\cdot\mathbf{x})$, where i is the imaginary unit and $\mathbf{k}$ is the wavevector, one obtains the dispersion relation $\rho^0(\omega)\omega^2 - \boldsymbol{\mu}^0 : \mathbf{k} \odot \mathbf{k} = 0$.

As it can be seen, no real wavevector can satisfy the dispersion relation if the effective mass is negative. This means that the band gaps of the hierarchical metamaterial are identified as the intervals of frequency in which $\rho^0(\omega) < 0$.

Example

The design of hierarchical LRM requires, besides the choice of the material and of the shape of the unit cell, also the selection of the number of masses and their distribution. As an example, we will consider a square unit cell, made of an epoxy matrix, rubber coatings and lead masses, see Fig. 1b. Typical values of the materials parameters are reported in Table 1.

Table1: *Properties of the constituent materials*

	E [MPa]	ν [-]	ρ [kg/m^3]
Matrix (epoxy)	3600	0.370	1180
Coatings (rubber)	0.118	0.469	1300
Rigid masses (lead)	14000	0.420	11340

We keep constant the total mass of coatings and resonant masses and we discuss the effect of changing the inclusions microstructure. Assuming $|Y_f| = 0.50\ell^2$ and $|Y_c| = 0.13\ell^2$, we obtain different unit cells (Fig. 3) by changing N and assuming that each sub-inclusion has the same mass. In the case of one, two and three rigid masses the effective mass density given by Eq. 9 is plotted against frequency in the left plates of Fig. 4a, 4b and 4c, respectively. Frequencies are

Materials Research Proceedings **26** (2023) 499-504 https://doi.org/10.21741/9781644902431-81

normalized with respect $\omega^* = \sqrt{\mu_c / \rho_c \ell^2}$. The dispersion curves, along the irreducible Brillouin zone of the unit cell (see Fig. 1c), are obtained by the numerical solution of Bloch-Floquet problems and are reported in the right plates of the same figures. The comparison shows the accuracy of the proposed homogenization approach for the prediction of the lowest band gaps (shaded in the figures) in the low-frequency regime.

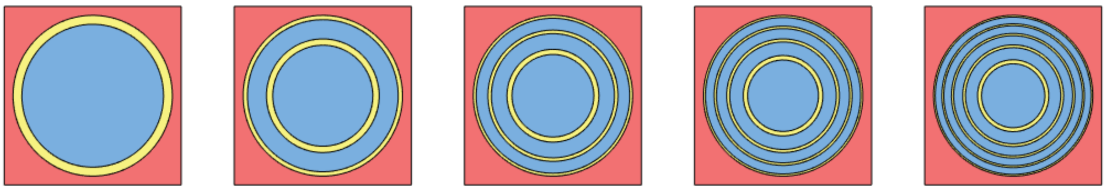

Figure 3: *First five hierarchy level considered.*

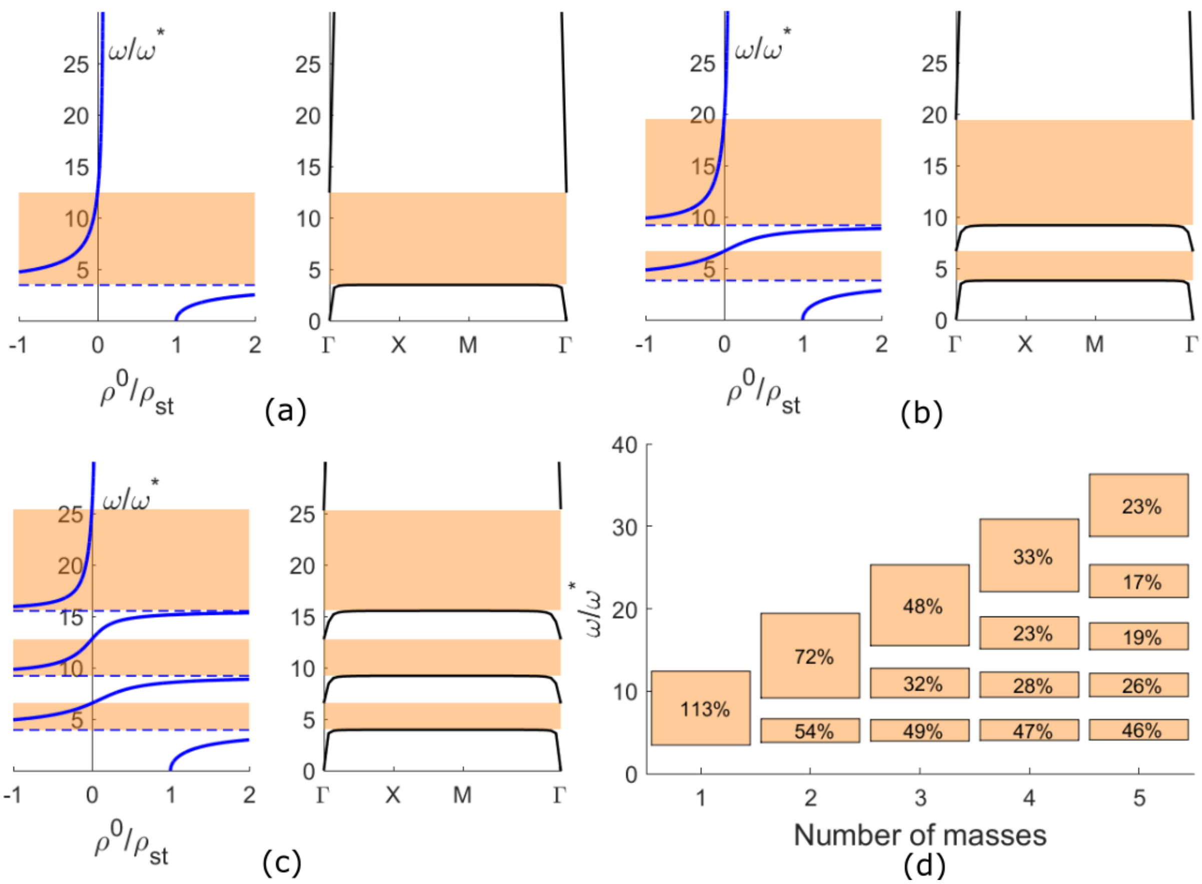

Figure 4: *Effective mass density against frequency (left) and numerical dispersion curves (right) in the case of one (a), two (b) and three (c) rigid masses. (d) Band gaps width as a function of the number of rigid masses.*

Figure 4d shows the width of band gaps for the first five hierarchical geometries with the corresponding gap mid-gap ratio $BG[\%] = 200(\omega_c - \omega_o)/(\omega_c + \omega_o)$, where ω_o and ω_c are the opening and closing frequency of the band gap. It can be observed that an additional band gap appears for each rigid mass considered, while the opening frequency of the first one is almost constant.

Materials Research Proceedings **26** (2023) 499-504 https://doi.org/10.21741/9781644902431-81

Conclusions

In this work, we studied the propagation of anti-plane shear waves in a continuous ternary locally resonant metamaterials, exhibiting a hierarchical mass-in-mass geometry, through asymptotic homogenization. In the simple case of concentric annular coatings and rigid masses we provide the expression of the effective dynamic mass density of the metamaterial up to the solution of a tridiagonal system, which has the same dimension of the number of sub-masses inside the inclusions.

The homogenized mass, which turns out to be frequency-dependent, allows for the prediction of the band gaps as intervals of frequency in which it becomes negative. This result has been validated by comparison with the band gaps obtained through numerical Bloch-Floquet analyses. This allow to perform parametric studies on the hierarchical metamaterial considered, which could be useful in their design phase.

The results obtained in this work can be easily generalized to wave propagation problems in plane strain conditions and for thin plates.

References

[1] C. Kittel. *Introduction to Solid State Physics 7th Ed.* Wiley, 1996.

[2] A. S. Phani, J. Woodhouse,N. A. Fleck. Wave propagation in two-dimensional periodic lattices. *J. Acoust. Soc. Am.*, 119(4):1995-2005, 2006. https://doi.org/10.1121/1.2179748

[3] C. Liu, C. Reina. Broadband locally resonant metamaterials with graded hierarchical architecture. *Journal of Applied Physics*, 123, 095108:1-10, 2018. https://doi.org/10.1063/1.5003264

[4] A. O. Oyelade, T. T. Akano. Graded hierarchical architecture metamaterial in vibration suppression. *UPB Scientific Bulletin*, *Series D: Mechanical Engineering*, 82(3):41-50, 2020.

[5] J. L. Auriault, G. Bonnet. Dynamique des composites élastiques périodiques. *Arch. Mech.*, 37:269-284, 1985.

[6] R. V. Craster, J. Kaplunov, A. V. Pichugin. High frequency homogenization for periodic media. *Proc. R. Soc. A Math. Phys. Eng. Sci.*, 466(2120):2341-2362, 2010. https://doi.org/10.1098/rspa.2009.0612

[7] C. Comi, J. J. Marigo. Homogenization Approach and Bloch-Floquet Theory for Band-Gap Prediction in 2D Locally Resonant Metamaterials. *Journal of Elasticity*, 139(1):61-90, 2020. https://doi.org/10.1007/s10659-019-09743-x

[8] C. Comi, M. Moscatelli, J. J. Marigo. Two scale homogenization in ternary locally resonant metamaterials. *Materials Physics and Mechanics*, 44(1):8-18, 2020.

[9] D. Faraci, C. Comi, J. J. Marigo. Band Gaps in Metamaterial Plates: Asymptotic Homogenization and Bloch-Floquet Approaches. *Journal of Elasticity*, 148(1):55-79, 2022. https://doi.org/10.1007/s10659-022-09879-3